

WIND TUNNEL INVESTIGATION AND ANALYSIS OF THE SM701 AIRFOIL

By Oran Nicks, Gregory Steen, Michael Heffner, David Bauer
Low Speed Wind Tunnel, Texas A & M University

Presented at the XXII OSTIV Congress, Uvalde, Texas, USA (1991)

ABSTRACT

A wind tunnel test was performed on a two-dimensional model of the SM701 airfoil designed for use on World Class gliders. The test covered a range of Reynolds Number conditions from one million to 2.5 million. Aerodynamic forces and moments were measured with an external balance. Wake-rake measurements of the two-dimensional drag were also made. Flow visualization techniques provided information on transition from laminar to turbulent flow. Post stall conditions were examined for both positive and negative angles of attack. Lift, drag, and pitching moment were analyzed and comparisons made with numerical predictions. The model was de-

signed, constructed, and the test conducted by students at Texas A&M University.

SYMBOLS:

A	Aspect ratio
C_{Di}	induced drag
C_f	friction coefficient
C_l	lift coefficient
$C_{l,max}$	maximum lift coefficient
ft	feet
Hz	Hertz

kPa	kiloPascals
KVA	kilovolt-amps
lbs	pounds
m	meters
mm	millimeters
N	Newtons
Pa	Pascals
psf	pounds per square foot
RN	Reynolds Number
RPM	revolutions per minute
X	longitudinal distance from test section center
Y	lateral distance from test section center
Z	vertical distance from test section center

BACKGROUND

The International Gliding Commission (IGC) of the Federation Aeronautique Internationale (FAI) initiated a design and prototype competition in the later part of 1989 for a new World Class glider to be used in international competition. Technical Specifications for this design and ground rules concerning the competition were announced worldwide by the FAI. The specifications were prepared after much deliberation by an international panel incorporating judgements that favor low cost, safety, suitable performance, and ease of handling that might encourage soaring on a worldwide basis.

The balanced characteristics chosen by the panel suggested the desirability of a high maximum lift coefficient, gentle stall and adequate L/D ratios at low Reynolds Numbers. Two experienced airfoil designers, Mr. Dan M. Somers and Dr. Mark D. Maughmer teamed to design a suitable airfoil, taking into account the compromises involved in World Class Technical Specifications. The SM701

airfoil was designed using the Eppler-Somers Airfoil Design Program. Its physical and design characteristics were then offered to all designers who might wish to employ this new section.

Because the analytical procedures are limited in the determination of some parameters such as maximum lift coefficient, characteristics after stall, determination of zero lift angle of attack, and pitching moment, it was proposed that experimental tests be conducted on a two-dimensional model of the SM701. A student project proposed by Texas A&M University was funded by NASA to perform this test using a modified wind tunnel model. The test was conducted and this report was prepared by a student team and an advisor at Texas A&M University under NASA Grant Number NAG1-1260-FDP. Mr. Dan Somers and Dr. Mark Maughmer provided consultation during the test along with lectures on the application of the Eppler-Somers airfoil design method.

FACILITY DESCRIPTION

The Texas A&M University Low Speed Wind Tunnel (TAMU-LSWT) is a self contained research facility located adjacent to Easterwood Airport in College Station, Texas.

The wind tunnel is of the closed circuit, single return type having a rectangular test section ten feet wide and seven feet high. Figure 1 presents a line drawing of the second floor of the building and a plan view of the wind tunnel circuit. Total circuit length at the centerline is 396 feet (120.7 m). The maximum diameter of 30 feet (9.14 m) occurs in the settling chamber. A single screen is located at the settling chamber entrance and a double screen just upstream of the contraction section to improve dynamic pressure uniformity and to reduce flow turbulence levels.

The contraction section which acts as a transition piece from circular to rectangular cross section is of reinforced concrete construction. Contraction ratio is 10.4 to 1 in a length of 30 feet (9.14 m).

Diffusion takes place immediately downstream of the test section in a concrete diffuser which also returns the flow to a circular section. The horizontal expansion angle is 1.43 degrees and the vertical 3.38 degrees in an overall length of 46.5 feet (14.17 m).

A 12.5 foot (3.81 m) diameter, four-blade Curtiss Electric propeller driven at 900 RPM by a 1250 KVA synchronous electric motor provides the air flow in the wind tunnel. Any desired test section dynamic pressure between zero and 100 pounds per square foot (0 - 4.79 kPa) can be obtained by proper blade pitch angle positioning.

Three separate studies were performed on tunnel parameters critical to the testing of a two dimensional laminar flow airfoil in preparation for the investigation of the SM701. These studies examined the test section freestream turbulence intensity,

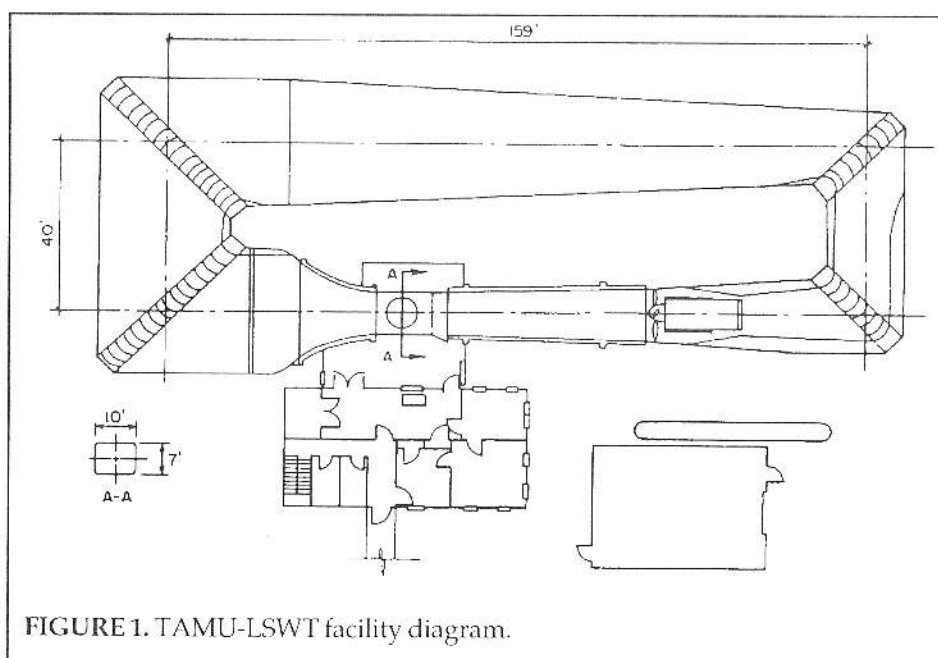


FIGURE 1. TAMU-LSWT facility diagram.

the floor and ceiling boundary layers, and the external balance system accuracy and repeatability.

Freestream turbulence intensity measurements were made at five different locations in the test section using a single component TSI hotwire and associated equipment. The data were not filtered or linearized, therefore the worst case is presented. Data were taken at each location in the test section at 10 different dynamic pressures. Each data point was obtained by analyzing 2048 samples acquired at 2000 Hz. Figure 2

presents a plot of turbulence intensity vs. dynamic pressure for each location. The turbulence intensity does not vary significantly with location but is a strong function of dynamic pressure. The SM701 airfoil was tested in the low turbulence intensity range of 4 psf (191 Pa) to 24 psf (1.15 kPa) dynamic pressure. The turbulence intensity ranges from approximately 0.3% to 0.9% in this range.

The test section floor and ceiling boundary layers were measured by using a twelve port boundary layer rake. The rake facilitated the measurement of the eleven total and one static pressures by the PSI-8400 pressure measurement system. The top total pressure port was located 3.60 inches (91.4 mm) above the surface and the static pressure port was located 4.10 inches (104.1 mm) above the surface. The boundary layer thickness was measured at the SM701 leading edge, quarter chord, and trailing edge locations as well as seven other locations on both the floor and the ceiling at ten different dynamic pressures. The displacement, momentum, and energy thicknesses were calculated based on the boundary layer surveys at each location. The boundary layer thicknesses on the floor and the ceiling were nearly identical. The boundary layer thickness, defined as the height above the surface where the local velocity reached 95% of the freestream velocity, grew from approximately 1.10 inches (28 mm) at the entrance to the test section to 2.55 inches (68 mm) at a point 42 inches (1.07 m) behind the center. The boundary layer thickness ranged from 1.85 inches (47 mm) at the leading edge location to 2.10 inches (53 mm) at the trailing edge location at a dynamic pressure of 30 psf (1.44 kPa).

The facility's six component pyramidal external balance was checked for repeatability and accuracy by repeatedly loading a single component with calibrated precision weights. These tests were done with both the tunnel drive motor off and on. The drag measurements were repeatedly accurate to within 0.05 lbs. (0.22 N) and the lift measurements were accurate to within 0.10 lbs. (0.44 N).

Both components were slightly better behaved with the drive motor on rather than off. It is believed this is due to the vibrations present in the system from the motor eliminating any sticking in the mechanical components of the balance system.

MODEL DESCRIPTION

The SM701 airfoil is a 16 percent thick, laminar flow airfoil designed for high maximum lift and low profile drag while exhibiting docile stall characteristics. The model constructed for this test had a span of 6.97 ft (2.17 m), a chord of 2.68 ft (0.82 m) and an area of 18.66 ft² (1.734 m²).

The model was built around an existing metal wing which was used as the backbone for the SM701 model. Foam was sanded to match the shape of the

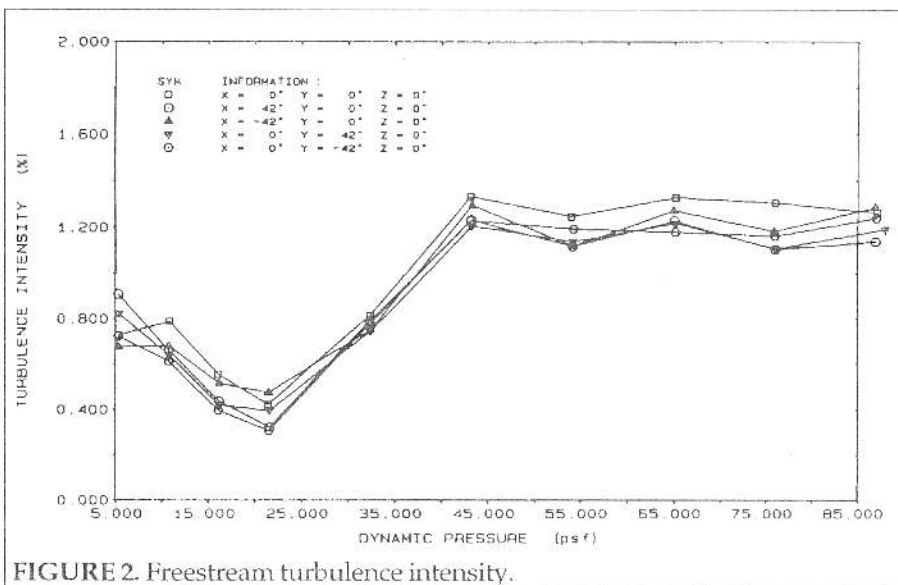


FIGURE 2. Freestream turbulence intensity.

upper and lower surfaces of the existing wing and then glued to the wing with an epoxy resin. Templates were generated on a computer and cut out of aluminum plates. These templates were mounted to each end of the foam covered wing. The foam was sanded down to the templates and covered with multiple layers of fiberglass. The final shape was obtained by using Bondo Body Filler to smooth out any irregularities in the airfoil shape. The model was sanded to a smooth finish and painted. After painting, the wing was polished by wet sanding with 600 grit sandpaper. Outer templates were then made from the model by using oversized profile shapes and filling in the gaps between the templates and the model with Bondo. From these templates, actual cross-sections were taken from three different stations along the span of the model. When compared with plots of the theoretical coordinates, some differences were noticed between the actual shape of the model and the theoretical shape. On the lower surface near the trailing edge, an error in thickness of 0.35% of the chord was observed between the two shapes. On the upper surface at approximately 5% from the leading edge, a maximum error of 0.28% was observed again in the thickness. In both cases, the model was thicker than the theoretical shape (Figure 3).

A steel mounting plate was attached to the model at one end and this plate was then bolted to the external balance. There was a 0.125 inch (3.12 mm) gap at the test section ceiling and the model extended into the floor. A floorplate with a 0.125 inch (3.12 mm) gap around the model was used.

Under high aerodynamic loadings the model was ob-

served to contact the floorplate so the gap was enlarged. This, however, allowed air from the balance room to be drawn into the test section and adversely affect the airflow around the model. Several floorplate configurations which attempted to eliminate this flow were tested and efforts were also made to close the model-ceiling gap. The final configuration that was tested is shown in Figure 4. A 0.125 inch (3.12 mm) ceiling gap was used to prevent interference during yaw sweeps. The bottom of the wing was placed 0.3125 inches (8 mm) above the floor and a spacer was placed between the model and the mounting plate with the floorplate fitting around the spacer. This configuration redirected any airflow from underneath the test section parallel to the floor.

TEST CONDITIONS

Angle of attack sweeps were run on the SM701 airfoil at four different dynamic pressures. Six component external balance data were taken at angles of attack from negative stall through positive stall in one degree increments. The set dynamic pressures were 4 psf (191.5 Pa), 9 psf (430.9 Pa),

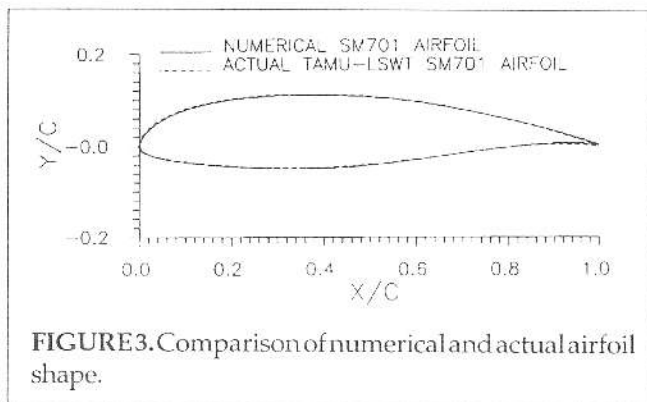


FIGURE 3. Comparison of numerical and actual airfoil shape.

15 psf (718.2 Pa), and 24 psf (1.149 kPa); these correspond to Reynolds Numbers of 1×10^6 , 1.5×10^6 , 2.0×10^6 , and 2.5×10^6 . The minimum Reynolds Number was limited by the ability to set and maintain a constant dynamic pressure in the test section. The maximum Reynolds Number was limited by the wind loads imposed on the external balance system.

Standard two-dimensional buoyancy, solid blockage, and wake blockage corrections as described in Reference 5 were applied to the force and moment data.

Drag on the SM701 was also measured by the momentum loss method. A traversing mechanism was installed in the tunnel which held a seven-hole pressure probe. The probe tip was

located one chord length behind the trailing edge of the airfoil. The total pressure was then read at 51 points in a 5 inch (127 mm) wide sweep using the PSI-8400 pressure measurement system. These 51 pressures were then integrated to obtain the section drag coefficient of the airfoil. The momentum loss method is very time consuming and was therefore run only on select cases. It was used to measure the laminar drag bucket of the airfoil. The particular cases run were: -4° , -2° , 0° , and 3° angle of attack at 1.0×10^6 , 1.5×10^6 , and 2.0×10^6 Reynolds Numbers, and -5° through 6° in 1° increments at a Reynolds Number of 2.5×10^6 .

Extensive flow visualization was also performed on the SM701. The method used was fluorescent oil painted on the surface of the airfoil. The test section was then bathed in ultraviolet light to show the contrast in the oil flow. The flow visualization was used to see laminar separation bubbles, transition, separation, flow angularity, and surface imperfections as well as examining the flow at the airfoil/floor and airfoil/ceiling junctures.

TEST RESULTS

VARIATION WITH REYNOLDS NUMBER

The lift coefficient and pitching moment coefficient were plotted versus angle of attack (Figures 5 and 6) showing the effects of Reynolds Number. These effects are small throughout the majority of the curve. They tend to be larger near stall. Near stall the lift coefficient increased with Reynolds Number. The maximum lift coefficient increased 1.54% between 1.0×10^6 and 2.5×10^6 Reynolds Number.

The lift coefficient was also plotted versus both the balance drag coefficient data and the momentum loss method drag coefficient data (Figures 7 and 8). The drag coefficient measured by both methods is the lowest at the high Reynolds Number.

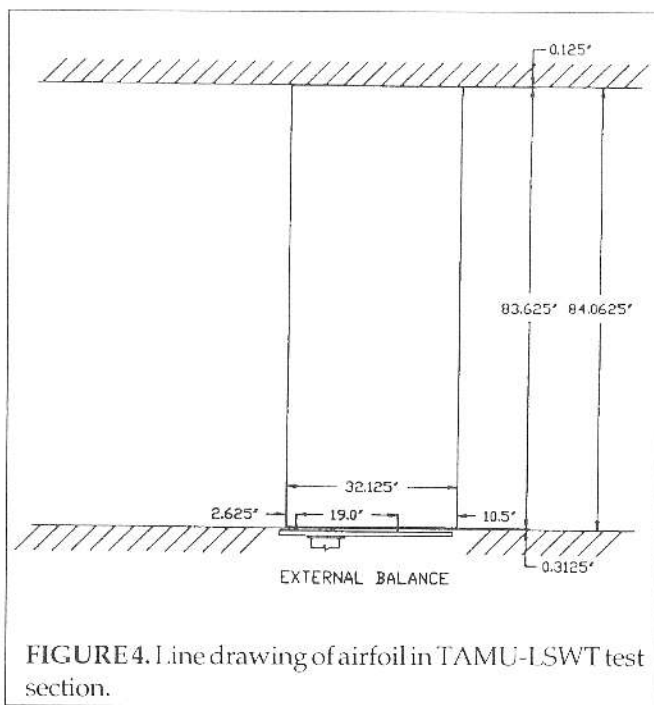


FIGURE 4. Line drawing of airfoil in TAMU-LSWT test section.

RESULTS AT 2.5 MILLION REYNOLDS NUMBER

The values for lift coefficient, both forms of drag coefficient, and pitching moment coefficient are presented along with the numerical predicted data and available experimental data acquired by D. Althaus for the 2.5×10^6 Reynolds Number case (Figures 9-11). The balance measured a maximum lift coefficient of 1.53 at an angle of attack of approximately 15° . The measured zero lift angle of attack was about 4° . The inverted maximum lift coefficient was -0.637 at -10° . The data

also show the positive stall to be quite gentle with no sudden or dramatic loss of lift. The inverted stall, however, was measured to be very hard with nearly a 40% drop in lift in just 1°. The pitching moment coefficient was fairly smooth and constant throughout the angle of attack range except at inverted stall. The values ranged from -0.112 at -1° to -0.074 at 15°. The pitching moment in inverted stall increased rapidly to nearly zero. A laminar drag bucket was measured by both the balance and the momentum loss method. The minimum drag coefficient measured by the balance was 0.0093 at -2°. The lowest drag part of the bucket was 3° wide while the entire bucket was 5° wide. The momentum loss method measured a minimum drag coefficient of 0.0062 at -1°.

The transition location was observed at various angles of attack through the use of the fluorescent oil flow visualization. The measured transition locations ranged from 64% aft of the leading edge at -2° to 12% aft at 14° on the upper surface. At -2° the transition location on the lower surface was measured to be approximately 60% aft of the leading edge.

DATA ANALYSIS

The lift coefficient versus angle of attack curve of the experimental data agrees well with the numerical predicted values through the low C_l range. The slope tends to flatten somewhat above a lift coefficient of 0.4. The maximum lift coefficient measured was 17% lower than predicted and approximately 7% lower than measured by Althaus. No predicted data were available for the inverted stall condition. The predicted zero lift angle of attack was -5.294° while the experiment showed this to be approximately -4°.

The drag coefficient measured by the balance was approximately 35% higher than the predicted and 27% higher than the momentum loss drag values through the laminar drag bucket. The measured balance drag near stall is very much higher than predicted. The momentum loss method drag coefficients were quite close to the predicted values and actually lower at some angles. These measured drag coefficients were extremely close to those measured by Althaus. The momentum loss method

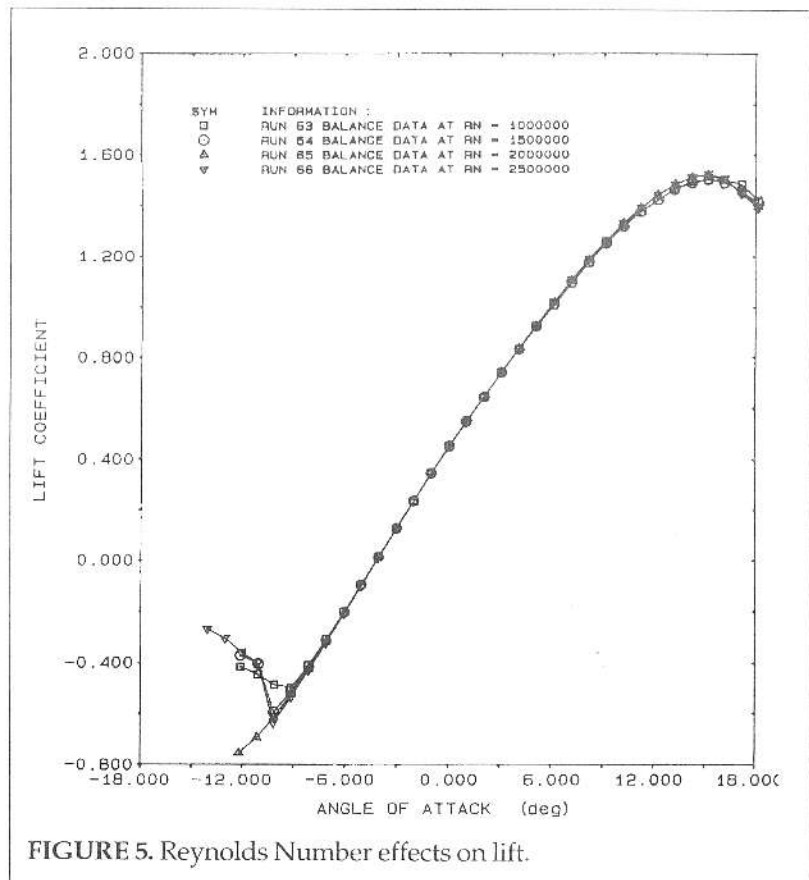


FIGURE 5. Reynolds Number effects on lift.

is generally a more accurate way to measure the two-dimensional section characteristics of an airfoil.

The pitching moment coefficient as measured by the balance was significantly lower than predicted. In general, the measured moment was about 35% lower.

The observance of the transition location tended to agree very well with the predicted values, especially at higher angle of attack. The observed transition was about 10%

forward of the predicted location near 0° angle of attack. The observed and predicted locations agreed within 3% at all other angles of attack.

Investigations were performed to consider possible three-dimensional, boundary layer, and reverse flow effects on the data due to the presence of gaps between the top of the model and the roof and the bottom of the model and the floor.

Knowing that floor and ceiling boundary layers interacted with the model, their effects on the model were also

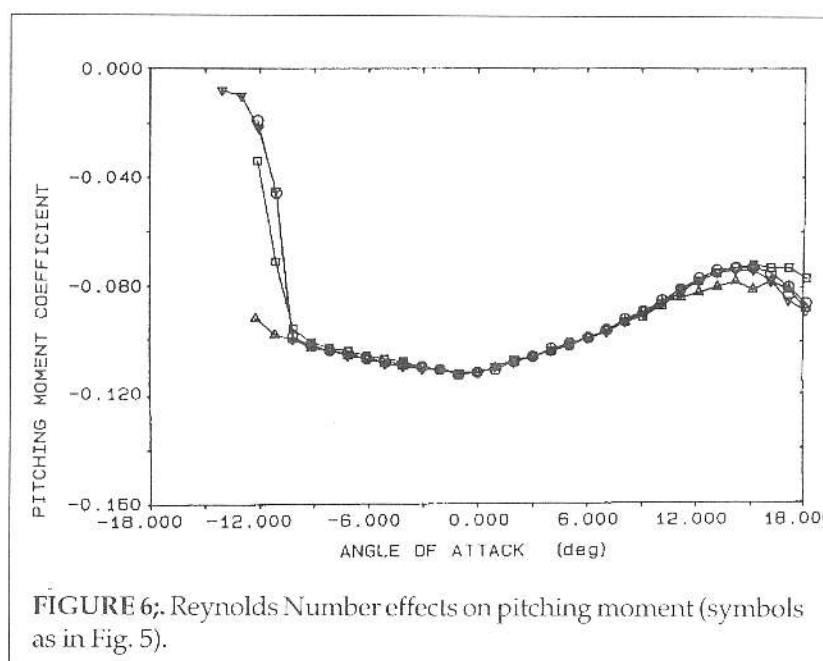


FIGURE 6: Reynolds Number effects on pitching moment (symbols as in Fig. 5).

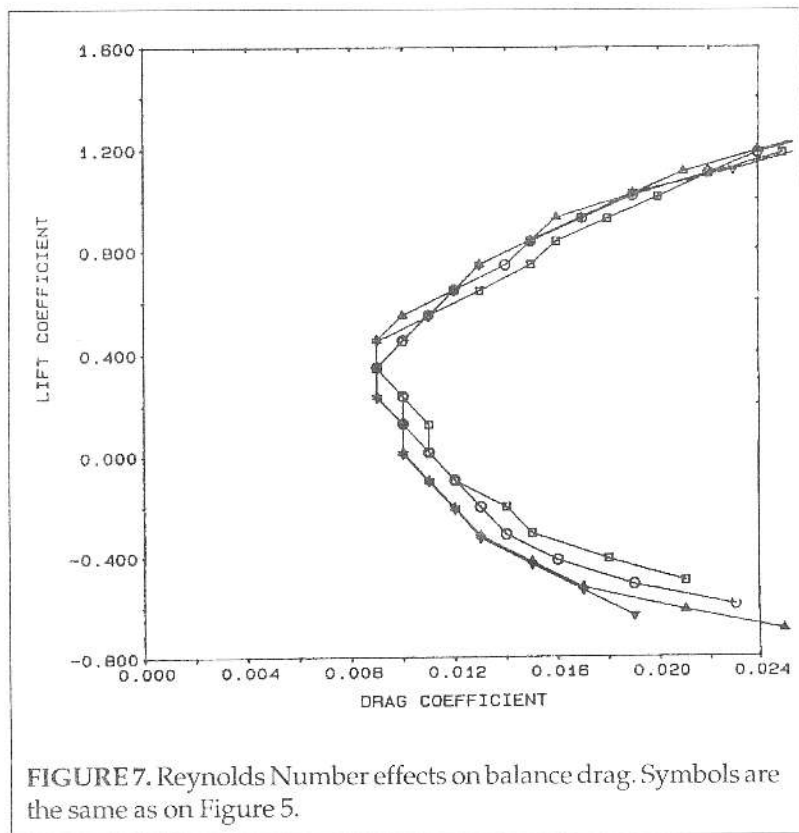


FIGURE 7. Reynolds Number effects on balance drag. Symbols are the same as on Figure 5.

studied. Previously performed boundary layer surveys provided values for the boundary layer thickness which interacted with the model, for both the floor and the ceiling. These thicknesses were weighted against the span of the model. For both the floor and the ceiling, the boundary layer thickness that interacted with the model was between 2% and 3% of the span. Flow visualization indicated that the other 94% to 96% of the model was unaffected by the boundary layer. The local dynamic pressures were found in the floor and ceiling boundary layers and multiplied by their respective weighted thicknesses. The same was done for the mid span of the model that was left

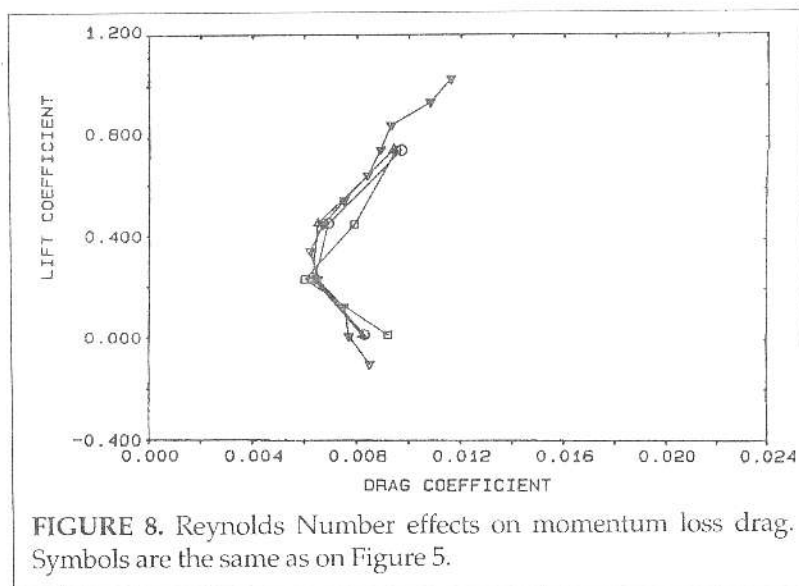


FIGURE 8. Reynolds Number effects on momentum loss drag. Symbols are the same as on Figure 5.

unaffected. When these three products were added together, the actual dynamic pressure can be adjusted for boundary layer effects. Results of this produced a reduction in dynamic pressure of no more than 2%.

Utilizing the flow visualization photographs, the areas on the wing near the floor and ceiling where separated and reverse flow existed were identified. It was assumed that these areas were not producing lift. The percentage of total effective area loss ranged from 1.94% at 2° angle of attack to 2.56% at 14°. The average loss over the entire angle of attack range was 2.26%.

Incorporating the above changes in the data would have resulted in proportional increases in the coefficients, but these corrections were not applied to the data presented.

DISCUSSION AND CONCLUSIONS

The results of a wind tunnel test on a two-dimensional model of the SM701 airfoil have been reported. Comparisons were made with theoretical calculations and other experimental results obtained earlier. A combination of direct measurements of lift, drag, and pitching moment are presented based on external balance measurements, suitably corrected for wind tunnel blockage and wall effects.

Boundary layer effects were considered and calculations were made to interpret these effects on the balance measurements. It was concluded that these and three-dimensional effects caused by the presence of a one-eighth inch gap between the upper end of the model and the ceiling moderated the values slightly; however, the simplified calculations to predict three-dimensional effects showed that the test produced results that were nearly two-dimensional. Wake rake data were obtained to survey the drag at low angles of attack where critical cruise conditions exist. Minimum drag coefficients of about 0.0062 compared with analytically predicted values of about 0.0055, being about 13% higher at the cruise condition. There do appear to be three-dimensional or boundary layer effects in the lift coefficient at high angles of attack. The maximum lift coefficient measured was approximately 17% lower than calculations predicted. The shape of the lift curve suggests some three-dimensional effects may have been present. The performance above stall indicates that the design goal of gentle stall characteristics was met.

Flow visualization techniques allowed the determination of transition from both the upper and lower surfaces at several Reynolds Numbers and angles of attack. These observations indicated that laminar flow was achieved over about 64% of the upper surface and 60% of the lower surface at -2° angle of attack and 2.5×10^6 Reynolds Number, closely approximating the predicted values.

The negative pitching moment of -0.100 is approximately 35% less than the predicted value.

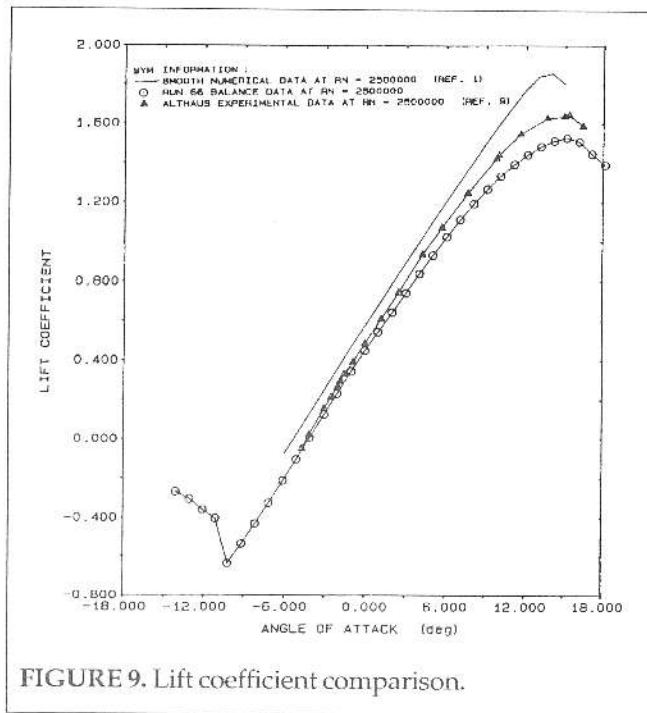


FIGURE 9. Lift coefficient comparison.

The zero lift angle of attack was about 1.3° less negative than predicted.

Measured values of stall lift coefficient at negative angles showed the C_{L_i} to be about -0.6 for three Reynolds Number cases. At a Reynolds Number of two million a negative lift coefficient of -0.77 was measured.

Together, all the experimental results obtained tend to verify the trends determined by analytical predictions. Because of the size of the model, there is greater confidence in the measurements at Reynolds Numbers of two million and above. These experimental data, combined with those reported in Reference 9 tend to support the expected

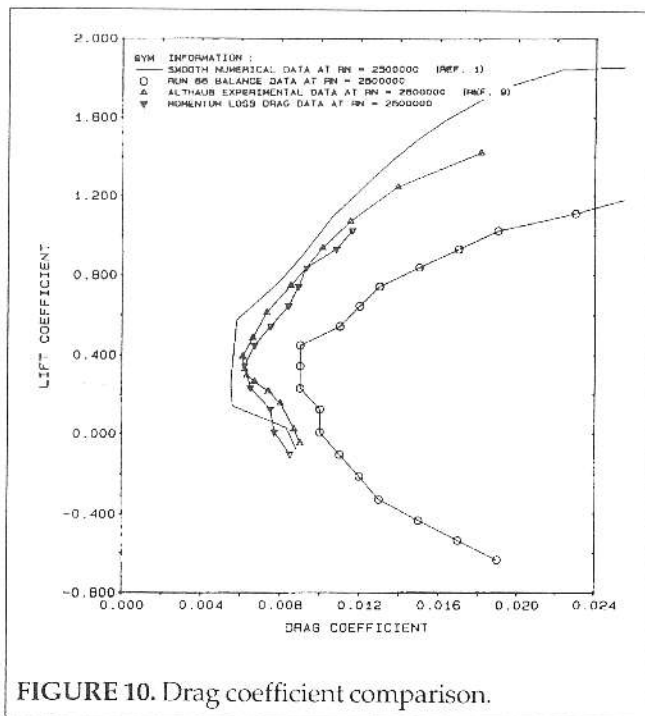


FIGURE 10. Drag coefficient comparison.

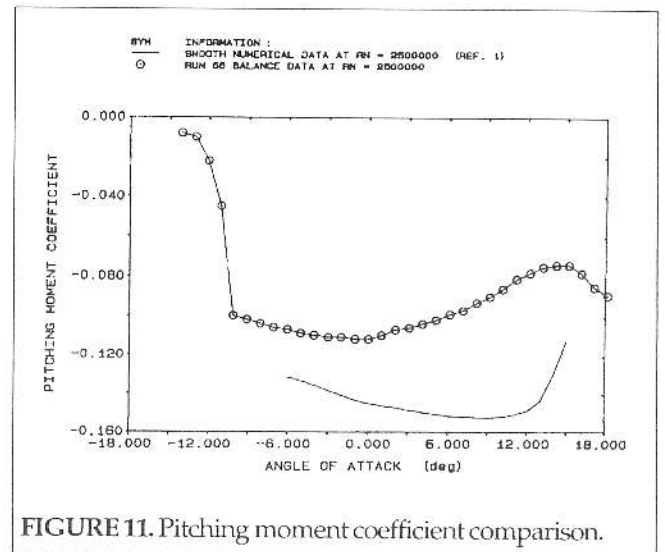


FIGURE 11. Pitching moment coefficient comparison.

performance of the airfoil as predicted by its designers.

REFERENCES:

1. Somers, Dan M.; and Maughmer, Mark D.: The SM701 Airfoil. Airfoils Incorporated, State College, Pennsylvania, 1990. Technical Soaring, Vol. 16, No. 3.
2. Morelli, Piero: The "World Class" Glider Design Competition. FAI Announcement. Technical Specifications, November, 1990.
3. Low Speed Wind Tunnel Facility Handbook. Texas A&M University, College Station, Texas, 1985.
4. Schlichting, Hermann: Boundary-Layer Theory. McGraw-Hill Book Company, New York, 1979.
5. Rae, William H.; and Pope, Alan: Low Speed Wind Tunnel Testing. John Wiley and Sons, New York, 1984.
6. Eppler, Richard: Airfoil Design and Data. Springer-Verlag, Berlin, 1990.
7. Hoerner, Sighard F.: Fluid-Dynamic Drag. Hoerner Fluid Dynamics, New Mexico, 1965.
8. Effects of End Plates on the Aerodynamic Characteristics of an Unswept Wing. NACA TN-2440, 1951.
9. Althaus, D.; and Wurz, W.: Wind Tunnel Tests of the SM701 Airfoil. Universitat Stuttgart, 1991.
10. Abbott, Ira H.; Von Doenhoff, Albert E.; and Stivers, Louis S., Jr.: Summary of Airfoil Data. NACA Rep. 824, 1945.